CHAPTER 11 HEALTH AREA

SYNTHESIS OF CHITOSAN SCAFFOLDS FOR TISSUE ENGINEERING USING SCHIFF REACTIONS

Gabriela Martínez-Mejía[1], Andrés Castell-Rodríguez[2], Rogelio Jiménez-Juárez[3], Mónica Corea[1*]

[1]Escuela Superior de Ingeniería Química e Industrias Extractivas, Instituto Politécnico Nacional, San Pedro Zacatenco, Gustavo A. Madero 07738, Ciudad de México, México.

[2]Departamento de biología celular y tisular, Universidad Nacional Autónoma de México, Facultad de Medicina, Circuito interior, Ciudad universitaria, Av. Universidad 3000, C.P. 04510, Ciudad de México, México

[3]Departamento de Química Orgánica, Escuela Nacional de Ciencias Biológicas, Instituto Politécnico Nacional, Prolongación de Carpio y Plan de Ayala s/n, Miguel Hidalgo, 11340, Ciudad de México, México.

* mcoreat@yahoo.com.mx, mcorea@ipn.mx

Abstract

Chitosan (CS) and glutaraldehyde (GA) hydrogels were synthesized for tissue engineering applications using a Schiff reaction. CS was reacted with GA (a cross-linker) at different concentrations, which were expressed as percentage of weigh. The effect of GA concentration on the swelling and rheological properties was evaluated. The Schiff crosslinking reaction was monitored by UV–vis spectroscopy (550 nm) to determine the reaction kinetic at 60 °C. The hydrogel structures were characterized by NMR, FT-IR, HR-MS and SEM, while the degree of cross-linking was examined with TGA-DA. The smaller pores and greatest swelling were found in hydrogels containing 10 wt% of GA. However, only the hydrogels with 2, 4 and 6 wt.% of GA displayed viable cells, indicating their *in vitro* cytocompatibility. The rheological studies showed that the values of the loss and storage modules in the hydrogels increased with temperature. Further research is needed to verify the adequacy of these hydrogels as a scaffold for tissue engineering *in vivo*.

Keywords: Scaffolds; Tissue engineering; Schiff reactions; chitosan; hydrogels

1. Introduction

The development of suitable scaffolds for tissue engineering is still one of the most important fields in regenerative medicine [1]. Creating scaffolds with the satisfactory physicochemical factors to sustain cell growth and tissue formation allow to regenerative medicine to improve, restore or replace the biological functions of damaged tissues and organs [2]. The scaffolds should serve as templates to guide adhesion, proliferation, differentiation and cell maturation. Furthermore, they must provide the cells a free space for vascularization, penetration and transfer of nutrients, oxygen and waste products [1, 3]. In other words, the scaffolds need to have appropriate mechanical properties and porous structures that allow the free diffusion of nutrients and waste. Also, the degradation process rate should be equal to the cellular growth rate [4, 5]. Essentially, scaffolds serve as an artificial extracellular matrix to offer structural support for the cells and free space for the flow of growth factors. The extracellular matrix consists of a crosslinked mesh between fibrous proteins and glycosaminoglycans (GAGs, such as heparan sulfate, chondroitin sulfate and keratan sulfate) to form proteoglycans [6]. These compounds have been reported for the regeneration of cartilage [7], bone [8], hair [9], nerves [10], tendons [10], ligaments [11], skin [12], fibrous tissue, blood vessels [13] and even heart and valves [14, 15].

The used synthetic polymers to prepare scaffolds are inexpensive but, they allow better functionality than natural polymers [16]. Furthermore, used polymeric materials to create structures in the form of scaffolds include the hydrogels [17], porous nanostructures and nanofibers [16]. Hydrogels are three-dimensional polymer networks able to swell and absorb a large amount of aqueous solution without losing their structure [17 - 19]. In addition, they can retain solvent at least 20 % of their own weight and swell significantly by absorbing water, followed by shrinking again after de-swelling. However, the process of cross-linking creates an insoluble network [20, 21].

Several monomers and crosslinking agents have been employed to synthesize hydrogels with a wide range of chemical compositions, many of which could be employed as scaffolds [22, 23]. There are several routes of synthesis of these platforms including Michael, Click and Schiff reactions. A Michael reaction involves the nucleophilic addition of a carbanion or a nucleophile (e.g., thiols and amines) to create a reaction with an α, β unsaturated carbonyl compound [24].

Hence, it is important to choose the type of reaction and depends on each special polymer. For example, chitosan (CS) has been used for the preparation of hydrogels via the Schiff base reaction.[16] CS is a linear heteropolymer of glucosamine and N-acetyl glucosamine residues (Figure 1) are obtained by the deacetylation of chitin. This weak base is soluble in acidic solution (pH 6.5) and insoluble in water and organic solvents [25 - 31]. It is biodegradable, biocompatible and non-toxic and exhibits mucoadhesive properties [20].

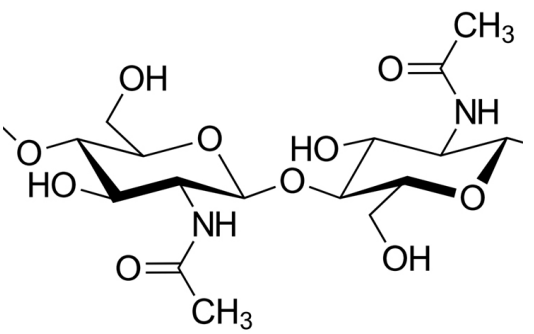

Figure 1. Chemical structure of chitosan.

2. Materials

CS (75% deacetylated) and 2,4-dinitrophenylhydrazine (DNP) (99%) were obtained from Sigma-Aldrich (Iceland), 99% acetic acid from J.T. Baker (Mexico), ethanol and dichloromethane from Alveg (Mexico), and 25 wt% GA from Merck (Germany). Distilled water grade II was used as solvent. The high glucose Dulbecco's modified Eagle's medium (DMEM), antibiotic-antimitotic 100X and fetal bovine serum (FBS) were purchased from Biowest (Mexico). Trypsin/EDTA solution and phosphate buffed saline (PBS, pH 7.4) were acquired from Gibco (Mexico). Calcein AM and ethidium homodimer (EthD-1) were provided by Life Technologies (USA).

3. Methods

3.1. *Synthesis of chitosan platforms*

The synthesis of CS scaffolds **3** (Scheme 1) started by dissolving 0.03 g CS **1** in 1% acetic acid aqueous solution. Different aliquots (0.05, 0.1, 0.15, 0.20 and 0.25 mL) of GA **2** (1.25% aqueous solution) were added drop wise and the reaction mixture was stirred for 2 h at 60 °C. Assays were performed by triplicate.

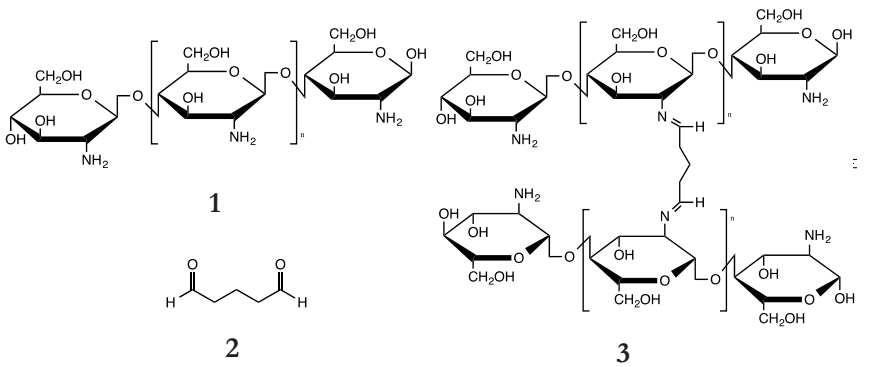

Scheme 1. Crosslinked hydrogels of chitosan-glutaraldehyde.

3.2. *Reaction kinetics*

The reaction between CS and GA was monitored by UV-vis spectroscopy at 550 nm in a PerkinElmer Lamda 25 UV-vis double beam spectrophotometer (Model 643, USA), taking samples every 5 min. Samples were extracted with methylene chloride under vigorous agitation and then, 2 mL of ethanol and 2 mL 2,4-dinitrophenylhydrazine of acid alcoholic solution (DNP) were added to the organic phase and the mixture was stirred[21]. The samples were analyzed by UV-vis spectroscopy.

3.3. *Nuclear Magnetic Resonance*

One-dimensional (1D) ^{1}H-NMR spectrum was recorded at 499.85 MHz on a Varian (now Agilent) NMR System 500 spectrometer (Agilent Technologies, Inc., Santa Clara, CA, USA). A sample of 30 mg hydrogel with GA at 10 wt% as well as its uncrossed fraction were dissolved in deuterated acetic acid/deuterated water (D_2O) (1:1). The non-crosslinked part of polymer was extracted washing the hydrogels by Soxhlet techniques using ethyl acetate as solvent. The ^{1}H NMR spectrum was recorded by employing a PRESAT pulse sequence to suppress the residual H_2O signal.

3.4. *Fourier Transform Infrared Spectroscopy (FT-IR)*

The fresh hydrogels were analyzed by Fourier transform infrared spectroscopy (FT-IR) in an infrared spectrophotometer, equipped with ATR in the mid-infrared region, from 400 to 4000 cm^{-1}.

3.5. *High-resolution mass spectrometry*

Fresh hydrogel was also examined by high-resolution mass spectrometry (HR-MS) on a mass spectrophotometer with micrOTOF II-Q and electrospray ionization (BrukerDaltonisc, Billerica, MA, USA).

3.6. *Scanning electron microscopy (SEM)*

The surface morphologies and cross sections of the chitosan scaffolds were coated with gold and observed with a field emission scanning electron microscope (JEOL JSM 6400) at an accelerating voltage of 5 kV.

3.7. *Thermogravimetric*

Derivate thermogravimetric analysis (DA-TGA) of the hydrogel was carried out on a 6000 PerkinElmer simultaneous thermal analyzer (Germany). The samples were heated from 25 to 500 °C at a rate of 10 °C/min under nitrogen atmosphere.

3.8. *Rheological analysis*

Rheological properties were evaluated with a Modular Compact Rheometer (model MCR 502, Anton Paar, Austria) using PP25 parallel plate geometry (25 mm diameter, 0°). The sample was placed in the center of the bottom plate. The upper plate was immediately lowered to a gap of 1 mm and the measurement was performed. The analysis was made at 30, 35 and 40 °C.

3.9. *Degree of cross-linking*

Fresh gel sample was washed in a Soxhlet system using ethyl acetate as solvent until constant weight. The degree of cross-linking was calculated gravimetrically using equation (1).

$$\%D = \frac{W_g}{W_0} \times 100 \qquad (1)$$

Where W_g is the weight of the sample after washing and W_0 is the initial weight.

3.10. *Cytotoxicity assay*

For testing the capacity of the scaffolds to support cell growth, primary cultures of human fibroblasts were used. These cells were obtained from the skin of healthy donors with prior informed consent. Thin layers samples of hydrogels were put on 0.5 x 0.5 mm coverslip frames, these were put in 48-well plates and sterilized by UV irradiation. Subsequently, 18 μL of cell suspension in DMEM were seeded onto hydrogel samples (5000 cells per sample) and incubated for 1 h at 37 °C, adding DMEM to the hydrogels. The cell-seeded hydrogels were cultivated for 1 week at 37 °C, changing the medium every 2 days. After 3 days, the cultivation medium was removed from the wells. The hydrogels were rinsed with PBS solution, stained with 1 mL of calcein/ethidium homodimer solution, and incubated for 1 h at 37 °C. With this dye, living cells fluoresce green and the nuclei of dead cells is red, thus providing the basis of the fluorescence live/dead assay.

4. Results

A series of hydrogels of CS and GA were synthesized (at 60 °C) by means of the Schiff base method, obtaining five concentrations of GA (2, 4, 6, 8 and 10 wt%) and therefore a range in the degree of cross-linking in the polymer. The synthesis was carried out by triplicate.

To know the progress of the reaction, the conversion of glutaraldehyde from the formation of hydrazones was determined. The reaction scheme 2 shows the carbonyl of glutaraldehyde **1** reacting with 2,4-dinitrophenylhydrazine **2** to form phenylhydrazones **3** obtaining a yellow complex. This is an indicator of the presence of aldehyde in the medium [32].

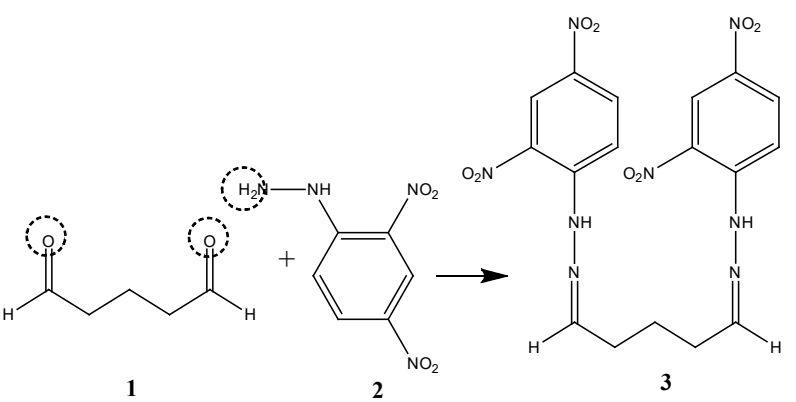

Scheme 2. Aldehyde identification reaction scheme.

The reaction progress was monitored for each hydrogel at 60 °C. The conversion data of GA as a function of time for hydrogels with a concentration of 2 wt% and 10 wt% are illustrative of the results as an example (Figure 2). The hydrogel containing GA at 2 wt% was completely consumed at 50 min of reaction. For the hydrogel with GA at 10 wt%, this occurred at 120 min of reaction.

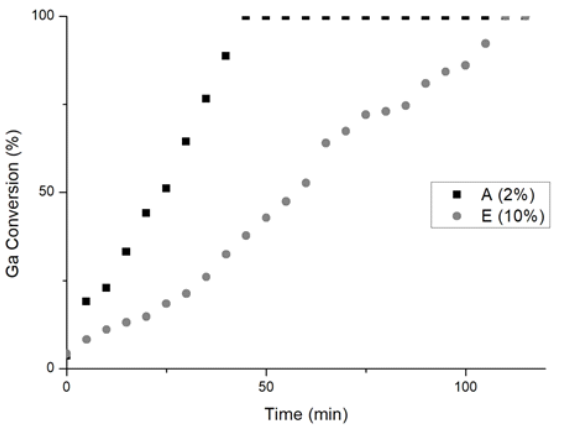

Figure 2. GA conversion of 2 wt% (■) and 10 wt% (●) hydrogel.

The reaction order was calculated from the GA conversion data for each hydrogel. Figure 3 shows the reaction order results for hydrogels with 2 wt% (■) and 10 wt% (●). It is possible to observe that the reaction between chitosan and glutaraldehyde has zero-order kinetic. That is, the reaction rate is independent of the concentration of reactants. Some authors have reported this reaction as spontaneous and immediate [19].

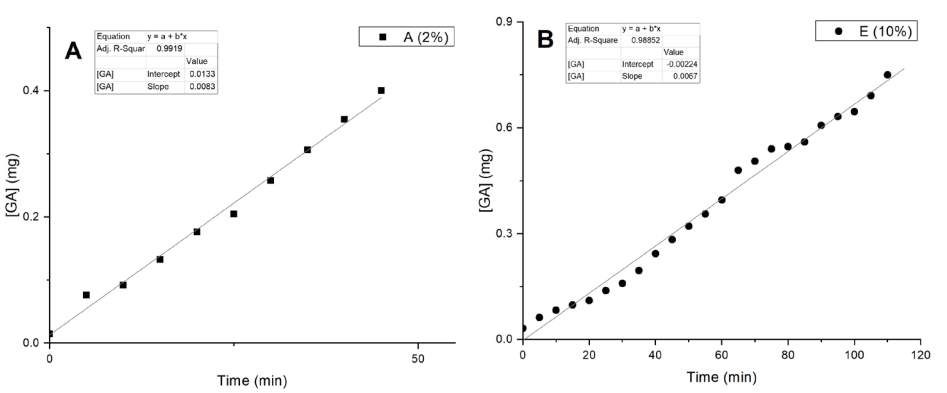

Figure 3. Reaction order of hydrogel at 2% by weight (■) and 10% by weight (●).

Spectra of ^{1}H NMR, result is shown for the crosslinking in the hydrogel containing GA at 10 wt% (Figure 4). A signal at δ=7.75 ppm was attributed to the imine protons for cross-linking between GA and CS (-N=CH-), in agreement with the report by Ali Reza Karimi [23]. A wide signal at δ=4.66 ppm corresponds to hydroxyl (-OH) groups in the CS chain, δ=3.16 ppm to oxygen base protons near hydroxyls (OH-CH-), and δ=1.83 ppm to methylene groups of the cross-linked glutaraldehyde chain.

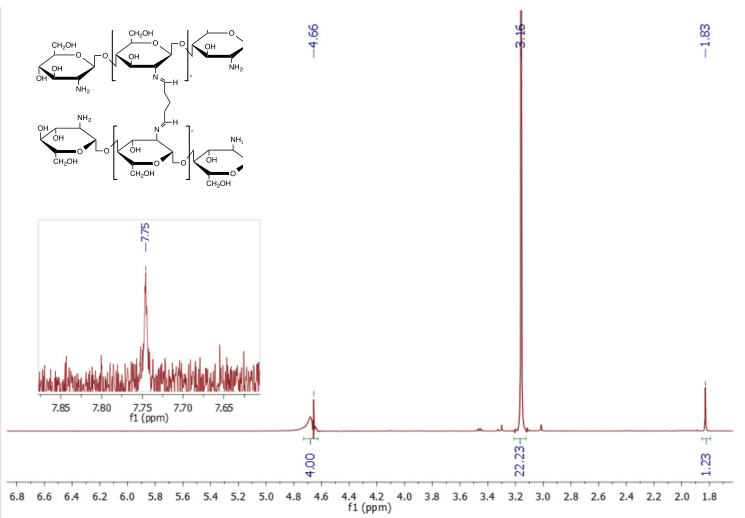

Figure 4. ^{1}H NMR of hydrogel at 10 wt%.

FT-IR analysis was carried out on fresh hydrogels with the crosslinking agent at 2 wt%, 6 wt% and 10 wt% (Figure 5). The absorption band at 1632 cm^{-1} corresponds to the stretching frequencies of the imine bond (HC=N-). This is

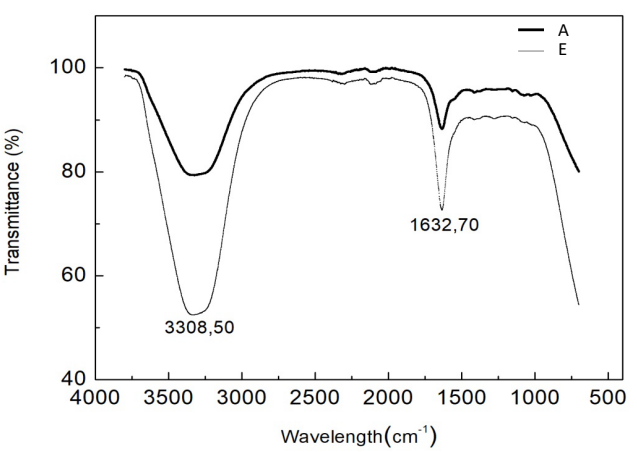

Figure 5. FT-IR spectra of chitosan-glutaraldehyde hydrogels containing the crosslinking agent at 2 wt% and 10 wt%.

according with a previous study, which employ the same reaction that assigned the imine group to 1568 cm^{-1} [26] and the overlapped stretching vibration of -N-H and –OH to 3308 cm^{-1} [26]. Both these signals presently increased when there was a greater cross-linking degree in the hydrogels.

HR-MS reveals a wide distribution of the molecular mass for each hydrogel (Figure 6). Some chains were found with high molecular weight and others with low molecular weight. The latter are attributed to a slow reaction that does not permit the fast growth of polymeric chains. This evidence corroborates the findings of the NMR spectrum in which residual CS and GA were detected.

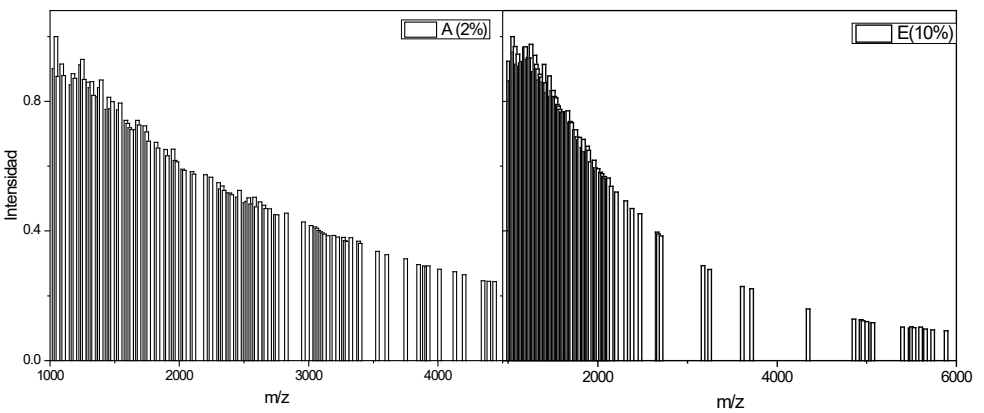

Figure 6. HR-MS spectra of chitosan-glutaraldehyde hydrogels containing the crosslinking agent at 2 wt% and 10 wt%.

The morphology of fresh and freeze-dried hydrogels was examined by SEM. Micrographs of the hydrogels containing 2 and 10 wt% of the crosslinking agent (Figure 7) show highly porous surfaces and the formation of flakes in fresh (Panel A) and lyophilized (Panel B) gels. There are studies that document the importance of a porous surface for cells to be implanted inside of the hydrogel and for nutrients to be able to flow to such cells, thus enabling tissue growth on the scaffold [3].

The DA-TGA test indicated that the hydrogel with the greatest concentration of GA decomposed at the highest temperature (Figure 8), caused by the greater crosslinking density and therefore a higher average molecular weight of the polymer chains. At first, the hydrogels with GA at 2, 4 and 6 wt.% presented the same weight loss at $25 < T/°C < 52$, attributed to dehydration of the material

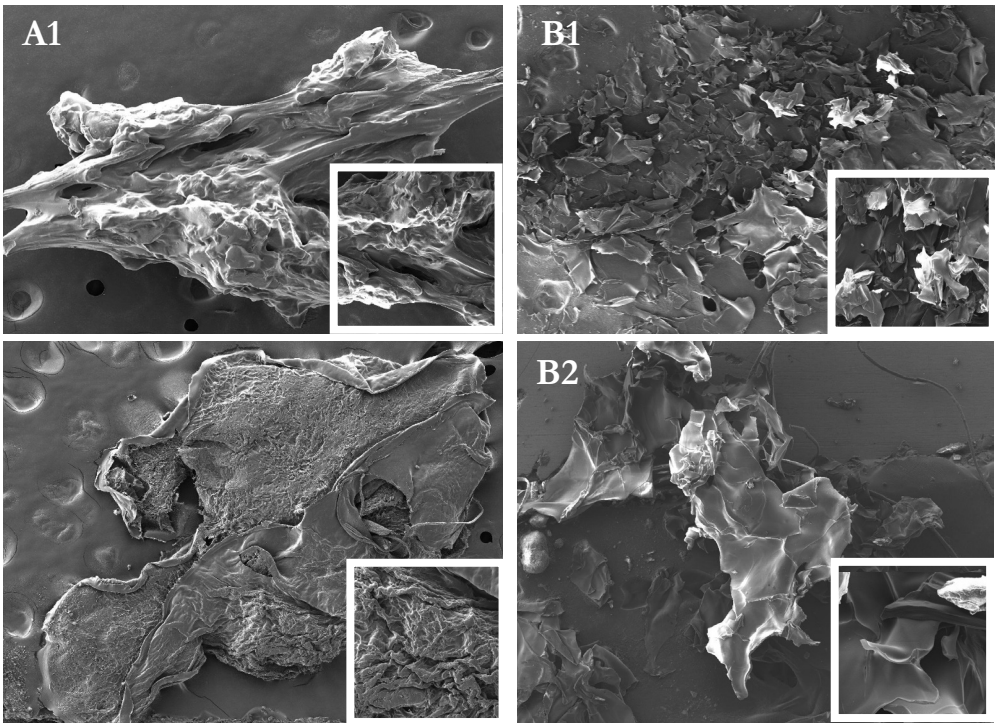

Figure 7. Microscopy images of the surfaces of hydrogels, both fresh (A) and lyophilized (B), containing 2 wt% and 10 wt% of the crosslinking agent.

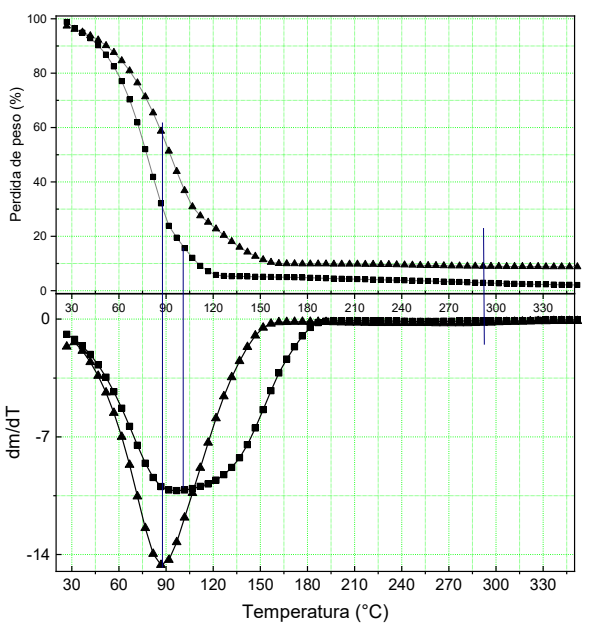

Figure 8. TGA and derivate analyses of crosslinked hydrogels with glutaraldehyde at 2 wt% (■) and 10 wt% (▲).

and the beginning of the decomposition of shorter chains. As the temperature approached 100 °C, there was a faster decomposition of the hydrogels containing GA at 2 and 6 wt.%. On the other hand, the hydrogel with GA at 10 wt.% di0d not accelerate its decomposition (due to its greater water retention).

The rheological properties of the hydrogels were studied by oscillatory rheology at 30, 35 and 40 °C. The storage modulus (*G´*) and loss modulus (*G´´*) were determined as a function of strain, (Figure 9), finding that *G'* was higher than *G´´*. Thus, the *G´* represents the elastic response of the sample, which is reportedly typical for gels or samples with a certain rigidity in their structure [33]. The shape of the storage modulus curve at low frequencies is typical of the shape of a polymer with mechanically weak cross-links [34].

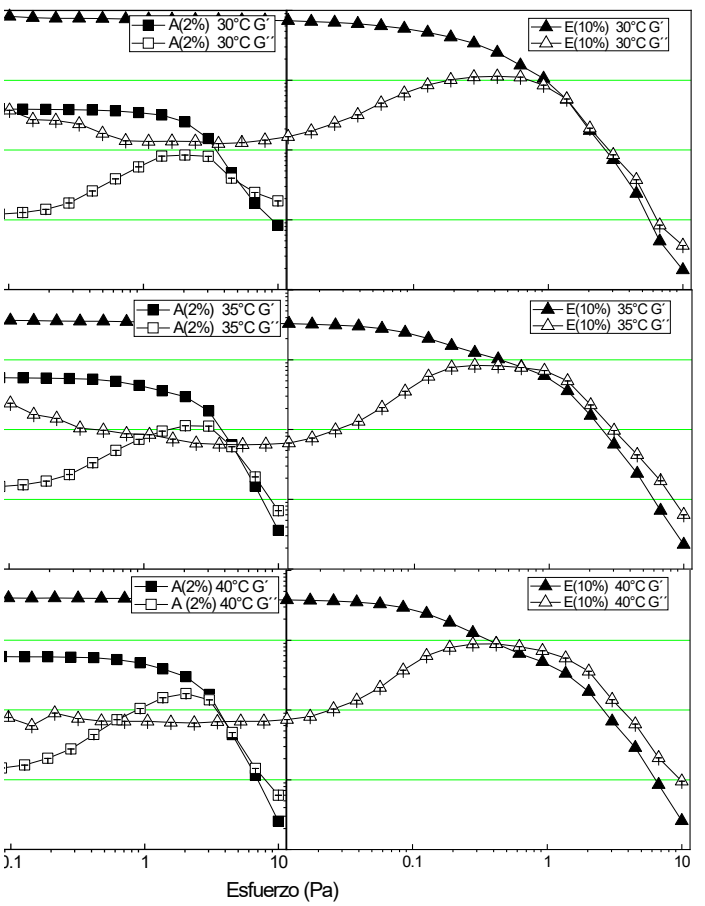

Figure 9. Storage modulus and loss modulus behavior of hydrogels with glutaraldehyde at 2 wt% (■) and 10 wt% (▲).

The degree of swelling of the material was determined by the quantity of water absorbed by the hydrogel. The percent of swelling was calculated as a function of the time. The material was immersed in water, using hydrogels with 2, 6 and 10 wt% of GA (Figure 10). The results reveal that the degree of crosslinking strongly influenced the swelling volume. That means, the material with the greatest degree of swelling was the material with the greatest percentage of the crosslinking agent (10 versus 2 wt%, respectively). Accordingly, the hydrogels containing 10 wt% GA absorbed 60% of water in the first 1.5 min, while the materials with 2 wt% only absorbed 20 %.

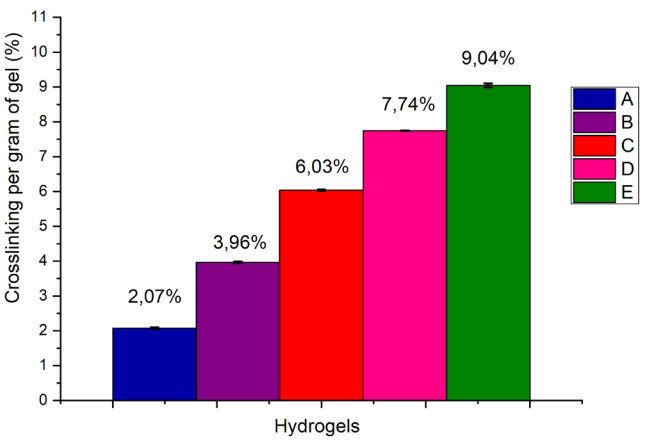

Figure 10. Crosslinking agent percentage of hydrogels at 2 wt% (■), 6 wt% (●) and 10 wt% (▲).

The cytocompatibility of CS-GA hydrogels with human fibroblasts was evaluated by using a live/dead cytotoxicity assay. The cells were seeded on the hydrogels and left for three days at 37 °C. Subsequently, the hydrogel platforms were stained with calcein/ethidium homodimer for the visualization of viable cells under an epifluorescence microscope (Figure 11). Viable fibroblasts were clearly seen in the platforms containing 2, 4 and 6 wt.% GA, indicating cytocompatibility at those concentrations. Viable cells can be appreciated alone or clusters, both on the surface of hydrogels. The hydrogels with GA at 8 and 10 wt% did not display cell viability, cells could not adhere perhaps due to the higher concentration of GA.

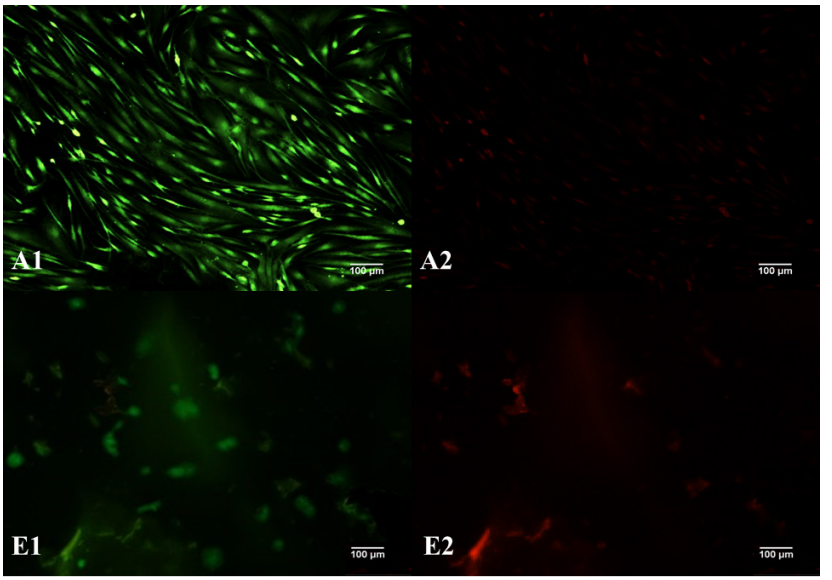

Figure 11. Fluorescence micrographs of the fibroblast cells onto hydrogels with the crosslinking agent at 2 wt% (A) and 10 wt% (E). Live cells are visible as green (1), dead cells are observed as red (2).

5. Conclusions

Novel hydrogels were synthesized by using Schiff reactions to cross-link CS with GA. Hydrogels having different concentrations of GA were tested to determine the effect on swelling and rheological properties. Examination was made of the degree of crosslinking bond formation (with TGA-DA) and of the presence of residual GA in the uncrossed part (with NMR). The reaction kinetic and reaction order assessed with UV-vis spectroscopy, showed a pseudo-zero order for the reaction. Moreover, the constant rate values were dependent on the concentration of GA. The rheological properties evidenced a decrease in the strain strength when a more rigid network is formed. There was a significant increase in the swelling capacity of the material with greater GA content, finding the best water absorption capacity at 10 wt%. However, only the hydrogels at 2, 4 and 6 wt% were cytocompatible. The results suggest that hydrogels consisting of CS cross-linked with GA could possibly provide an adequate scaffold for tissue engineering. Further research is needed to explore the in vivo plausibility of such a scaffold.

Acknowledgement

Thanks for the financial support provided by the ENCB CASCO-IPN.

References

1. Demina, T. S., Zaytseva-Zotova, D. S., Akopova, T. A., Zelenetskii, A. N., & Markvicheva, E. A. (2017). Macroporous hydrogels based on chitosan derivatives: Preparation, characterization, and in vitro evaluation. *Journal of Applied Polymer Science, 134*(17-19). https://doi.org/10.1002/app.44651

2. Scaplehorn, N. (2012). Regenerative medicine. *Cell, 149*(727–729). https://doi.org/10.1016/j.cell.2012.04.022

3. Kim, S., Kawai, T., Wang, D., & Yang, Y. (2016). Engineering a dual-layer chitosan–lactide hydrogel to create endothelial cell aggregate-induced microvascular networks in vitro and increase blood perfusion in vivo. *ACS Applied Materials & Interfaces, 8*(19245–19255). https://doi.org/10.1021/acsami.6b04431

4. Jin, R., Moreira Teixeira, L. S., Krouwels, A., Dijkstra, P. J., van Blitterswijk, C. A., Karperien, M., et al. (2010). Synthesis and characterization of hyaluronic acid-poly(ethylene glycol) hydrogels via Michael addition: An injectable biomaterial for cartilage repair. *Acta Biomaterialia, 6*(1968–1977). https://doi.org/10.1016/j.actbio.2009.12.024

5. Lee, K. Y., & Mooney, D. J. (2001). Hydrogels for tissue engineering. *Chemical Reviews, 101*(1869–1879). https://doi.org/10.1021/cr000108x

6. Ahadian, S., Sadeghian, R. B., Salehi, S., Ostrovidov, S., Bae, H., Ramalingam, M. et al. (2015). Bioconjugated hydrogels for tissue engineering and regenerative medicine. *Bioconjugate Chemistry, 26*(1984–2001). https://doi.org/10.1021/acs.bioconjchem.5b00360

7. King-Martínez, A. C., Doger-Echegaray, P., & Hoyo-Pérez, L. I. (2020). Identificación por imágenes del paciente con pie diabético del tipo de lesiones que requirieron o requerirán amputación. *Acta Ortopédica Mexicana, 34*(2), 77–80. https://doi.org/10.35366/95318

8. Montoya, A., Gallardo-Rincón, H., Silva-Tinoco, R., García-Cerde, R., Razo, C., Ong, L. et al. (2023). Type 2 diabetes epidemic in Mexico. Burden of disease 1990-2021 analysis and implications for public policies. *Gaceta Médica de México, 159*(474–486). https://doi.org/10.24875/GMM.23000378

9. Holl, J., Kowalewski, C., Zimek, Z., Fiedor, P., Kaminski, A., Oldak, T. et al. (2021). Chronic diabetic wounds and their treatment with skin substitutes. *Cells, 10*(3), 655. https://doi.org/10.3390/cells10030655

10. Funakoshi, T., Majima, T., Iwasaki, N., Suenaga, N., Sawaguchi, N., Shimode, K. et al. (2005). Application of tissue engineering techniques for rotator cuff regeneration using a chitosan-based hyaluronan hybrid fiber scaffold. *The American Journal of Sports Medicine, 33*, 1193–1201.
https://doi.org/10.1177/0363546504272689

11. Funakoshi, T., Majima, T., Iwasaki, N., Yamane, S., Masuko, T., Minami, A. et al. (2005). Novel chitosan-based hyaluronan hybrid polymer fibers as a scaffold in ligament tissue engineering. *Journal of Biomedical Materials Research Part A, 74*, 338–346.
https://doi.org/10.1002/jbm.a.30237

12. Wu, R. D. (2009). Application of synthetic and natural scaffold materials in skin tissue engineering. *Journal of Clinical Rehabilitation Tissue Engineering Research, 12*, 2317–2320.

13. Scherner, M., Reutter, S., Klemm, D., Sterner-Kock, A., Guschlbauer, M., Richter, T. et al. (2014). In vivo application of tissue-engineered blood vessels of bacterial cellulose as small arterial substitutes: Proof of concept? *Journal of Surgical Research, 189*, 340–347.
https://doi.org/10.1016/j.jss.2014.02.011

14. Blan, N. R., & Birla, R. K. (2008). Design and fabrication of heart muscle using scaffold-based tissue engineering. *Journal of Biomedical Materials Research Part A, 86*, 195–208.
https://doi.org/10.1002/jbm.a.31642

15. Fallahiarezoudar, E., Ahmadipourroudposht, M., Idris, A., & Yusof, N. M. (2015). A review of: Application of synthetic scaffold in tissue engineering heart valves. *Materials Science and Engineering C, 48*, 556–565.
https://doi.org/10.1016/j.msec.2014.12.016

16. Yang, J. A., Yeom, J., Hwang, B. W., Hoffman, A. S., & Hahn, S. K. (2014). *In situ*-forming injectable hydrogels for regenerative medicine. *Progress in Polymer Science, 39*, 1973–1986.
https://doi.org/10.1016/j.progpolymsci.2014.07.006

17. Miranda, D. G., Malmonge, S. M., Campos, D. M., Attik, N. G., Grosgogeat, B., & Gritsch, K. J. (2016). A chitosan-hyaluronic acid hydrogel scaffold for periodontal tissue engineering. *Journal of Biomedical Materials Research Part B: Applied Biomaterials, 104*, 1691–1702.
https://doi.org/10.1002/jbm.b.33516

18. Ray, M., Pal, K., Anis, A., & Banthia, A. K. (2010). Development and characterization of chitosan-based polymeric hydrogel membranes. *Designed Monomers and Polymers, 13*, 193–206.
https://doi.org/10.1163/138577210X12634696333479

19. Buwalda, S. J., Boere, K. W. M., Dijkstra, P. J., Feijen, J., Vermonden, T., & Hennink, W. E. (2014). Hydrogels in a historical perspective: From simple networks to smart materials. *Journal of Controlled Release, 190*, 254–273.
20. https://doi.org/10.1016/j.jconrel.2014.03.052

21. Santillán, R., Nieves, E., Alejandre, P., Pérez, E., Del Río, J. M., & Corea, M. (2014). Comparative thermodynamic study of functional polymeric latex particles with different morphologies. *Colloids and Surfaces A: Physicochemical and Engineering Aspects, 444*, 189–208. https://doi.org/10.1016/j.colsurfa.2013.12.004

22. Shu, X. Z., Liu, Y., Palumbo, F. S., Luo, Y., & Prestwich, G. D. (2004). In situ crosslinkable hyaluronan hydrogels for tissue engineering. *Biomaterials, 25*, 1339–1348. https://doi.org/10.1016/j.biomaterials.2003.08.014

23. Thürmer, M. B., Diehl, C. E., Brum, F. J. B., & dos Santos, L. A. (2014). Preparation and characterization of hydrogels with potential for use as biomaterials. *Materials Research, 17*, 109–113. https://doi.org/10.1590/1516-1439.223613

24. Kopeček, J. (2007). Hydrogel biomaterials: A smart future? *Biomaterials, 28*, 5185–5192. https://doi.org/10.1016/j.biomaterials.2007.07.044

25. Jansen, L. E., Negrón-Piñeiro, L. J., Galarza, S., & Peyton, S. R. (2018). Control of thiol-maleimide reaction kinetics in PEG hydrogel networks. *Acta Biomaterialia, 70*, 120–128. https://doi.org/10.1016/j.actbio.2018.01.043

26. Desai, R. M., Koshy, S. T., Hilderbrand, S. A., Mooney, D. J., & Joshi, N. S. (2015). Versatile click alginate hydrogels crosslinked via tetrazine–norbornene chemistry. *Biomaterials, 50*, 30–37. https://doi.org/10.1016/j.biomaterials.2015.01.048

27. Karimi, A. R., Rostaminejad, B., Rahimi, L., Khodadadi, A., Khanmohammadi, H., & Shahriari, A. (2018). Chitosan hydrogels cross-linked with tris (2-(2-formylphenoxy) ethyl) amine: Swelling and drug delivery. *International Journal of Biological Macromolecules, 118*, 1863–1870. https://doi.org/10.1016/j.ijbiomac.2018.07.037

28. Giri, T. K., Thakur, A., Alexander, A., Ajazuddin, Badwaik, H., & Tripathi, D. K. (2012). Modified chitosan hydrogels as drug delivery and tissue engineering systems: Present status and applications. *Acta Pharmaceutica Sinica B, 2*, 439–449. https://doi.org/10.1016/j.apsb.2012.07.004

29. Arakawa, C., Ng, R., Tan, S., Kim, S., Wu, B., & Lee, M. (2017). Photopolymerizable chitosan–collagen hydrogels for bone tissue engineering. *Journal of Tissue Engineering and Regenerative Medicine, 11*, 164–174. https://doi.org/10.1002/term.1896

30. Croisier, F., & Jérôme, C. (2013). Chitosan-based biomaterials for tissue engineering. *European Polymer Journal, 49*, 780–792. https://doi.org/10.1016/j.eurpolymj.2012.12.009

31. Duan, J., Liang, X., Cao, Y., Wang, S., & Zhang, L. (2015). High strength chitosan hydrogels with biocompatibility via new avenue based on constructing nanofibrous architecture. *Macromolecules, 48*, 2706–2714. https://doi.org/10.1021/acs.macromol.5b00117

32. Franzén, H. M., Draget, K. I., Langebäck, J., & Nilsen-Nygaard, J. (2015). Characterization and properties of hydrogels made from neutral soluble chitosan. *Polymers, 7*, 373–389. https://doi.org/10.3390/polym7030373

33. Jones, L., Kinney, C., & Seligman, R. (1961). The reaction of 2,4-dinitrophenylhydrazine with some dicarbonyl compounds and α-substituted carbonyl compounds. *Journal of the American Chemical Society, 26*, 228–232. https://doi.org/10.1021/jo01060a056

34. Mourycová, J., Datta, K. K. R., Procházková, A., Plotěná, M., Enev, V., Smilek, J. et al. (2018). Facile synthesis and rheological characterization of nanocomposite hyaluronan-organoclay hydrogels. *International Journal of Biological Macromolecules, 111*, 680–684. https://doi.org/10.1016/j.ijbiomac.2018.01.068

35. Klompen, E. T. J. (2005). *Mechanical properties of solid polymers: Constitutive modelling of long and short term behaviour*. Eindhoven: Technische Universiteit Eindhoven.